Quasiperiodic and chaotic discrete breathers in a parametrically driven system without linear dispersion

P. Maniadis[1] and T. Bountis[2]
[1]*Max-Planck-Institut für Physik Komplexer Systeme, Nöthnitzer Str. 38, D-01187 Dresden, Germany*
[2]*Department of Mathematics and Center of Research and Applications of Nonlinear Systems, University of Patras, 26500 Patras, Greece*

(Received 7 December 2005; revised manuscript received 24 February 2006; published 28 April 2006)

We study a one-dimensional lattice of anharmonic oscillators with only quartic nearest-neighbor interactions, in which discrete breathers (DB's) can be explicitly constructed by an exact separation of their time and space dependence. Introducing parametric periodic driving, we first show how a variety of such DB's can be obtained by selecting spatial profiles from the homoclinic orbits of an invertible map and combining them with initial conditions chosen from the Poincaré surface of section of a simple Duffing's equation. Placing then our initial conditions at the center of the islands of a major resonance, we demonstrate how the corresponding DB can be stabilized by varying the amplitude of the driving. We thus discover around elliptic points a large region of *quasiperiodic* breathers, which are stable for very long times. Starting with initial conditions close to the elliptic point at the origin, we find that as we approach the main chaotic layer, a quasiperiodic breather either destabilizes by delocalization or turns into a *chaotic* breather, with an evidently broadbanded Fourier spectrum before it collapses. For some breather profiles stable quasiperiodic breathers exist all the way to the separatrix of the Duffing equation, indicating the presence of large regions of tori around the DB solution in the multidimensional phase space. We argue that these strong localization phenomena are due to the absence of phonon resonances, as there are no linear dispersion terms in our lattices. We also show, however, that these phenomena persist in more realistic physical models, in which weak linear dispersion is included in the equations of motion, with a sufficiently small coefficient.

DOI: 10.1103/PhysRevE.73.046211 PACS number(s): 05.45.−a, 63.20.Pw, 63.20.Ry

I. INTRODUCTION

Localized oscillations in one-dimensional Hamiltonian lattices have been known to exist for a long time [1]. It was not, however, until their existence was rigorously proved in [2] that an explosive amount of work began to be published concerning their properties, structure, and possible applications [3–9].

These oscillations are periodic, with an exponentially localized profile, and as they occur in discrete systems, they have been termed *discrete breathers* (DB's), in reference to similar solutions called breathers first discovered in completely integrable nonlinear wave equations [10]. DB's belong to a class we may call *simple periodic orbits* of *N*-degrees-of-freedom Hamiltonian systems [11], where all rotation numbers are equal to unity, such as, e.g., in the case of nonlinear normal modes of the famous Fermi-Pasta-Ulam (FPU) problem [12,13].

Soon after the first developments, the question of the existence of quasiperiodic and even chaotic breathers arose in the study of Hamiltonian lattices. In particular, Johansson and Aubry [14] studied them in the discrete nonlinear Schrödinger (DNLS) equation, where a second frequency can be exactly imposed by the factor $\exp(i\omega t)$ multiplying a DB solution oscillating with frequency ω_b. A more rigorous approach was developed later by Bambusi and Vella [15], who used Nekhoroshev theory and the anticontinuum limit to construct quasiperiodic breathers in Hamiltonian systems possessing some additional integrals independent of the Hamiltonian. In these cases, it was shown that resonances with the linear spectrum can be avoided, as it is precisely the occurrence of such resonances that leads to the delocalization and eventual collapse of a breather [16,17].

Chaotic breathers have also been reported in the literature, primarily in connection with the problem of energy equipartition in FPU lattices [18–21]. In these studies, chaotic breathers were observed to occur as highly localized structures, which travel erratically along the whole lattice, until they eventually collapse due to energy exchange with the linear modes.

Since resonances with the linear spectrum appear to be so important to the persistence of localized structures, we thought that it might be a good idea to examine their importance indirectly, by considering an example where phonons are totally *absent*. We therefore study in this paper a one-dimensional lattice described by the Hamiltonian

$$H = \sum_n \left\{ \frac{1}{2}\dot{u}_n + V(u_n) + \frac{K}{4}(u_{n+1} - u_n)^4 \right\}, \qquad (1)$$

which is free from linear dispersion as it involves only quartic nearest-neighbor interactions. This lattice was also studied by Comte [22], who showed the existence of "compacton" breathers for a special choice of the on-site potential $V(u_n)$ by separating exactly the time and space dependence of the breather solutions. In fact, Kivshar [23] was the first to predict the occurrence of such compact structures in the presence of only anharmonic nearest-neighbor coupling and this was later confirmed numerically by Tchofo Dinda [24] on a Klein-Gordon lattice with a quartic on-site potential.

In the continuum limit, a generalized Konteweg–de Vries (KdV) equation was used by Rosenau and co-workers [25] to describe the existence of compact solitons. The substitution of the linear with a nonlinear dispersion was justified by the disentanglement of the parameters related with the characteristic length and nonlinear interactions on the system. The modified KdV equation proposed by Rosenau was proven to support compact solitons in the continuum limit. The different length scales in the magnetization that appear in anisotropic ferromagnetic systems can affect the balance between linear and nonlinear dispersion [26]. In the case of an Ising ferromagnet, the linear dispersion of the Landau-Lifshitz equation drops to zero and the magnetic solitons compactify. A mechanical analog, where the linear dispersion is considered to be very small compared to the nonlinear dispersion, was also proposed by Dusuel *et al.* in [27].

Breathers with an exactly compact profile, however, are not expected to exist generically. In fact, such structures are often called "compact like," as they are commonly found to obey superexponential decay laws [28]. More recently, Gorbach and Flach [29] used Hamiltonian (1), with the coupling term in the sum replaced by

$$\frac{K}{4l^s}\sum_{l>0}\{(u_{n+l}-u_n)^4+(u_{n-l}-u_n)^4\}, \tag{2}$$

to study the effect of long-range interactions on different breather profiles and showed how compactness can break down at certain well-defined crossover length scales.

In this paper, we use again the exact separation of the solutions into the product of a temporal and a spatial part, as demonstrated in [4,23,29], to obtain, in Sec. II, DB's of a Hamiltonian lattice (1), whose substrate potential is a "soft" quartic

$$V(x)=\frac{1}{2}x^2-\frac{1}{4}x^4. \tag{3}$$

In cases where the DB's are linearly unstable, we introduce an oscillatory modulation in the coefficient of quadratic term in Eq. (3), replacing it by $\frac{1}{2}x^2[1+\epsilon\cos(\omega_d t)]$. This periodic control introduces new parameters in the problem, which can now be varied accordingly to generate new kinds of breathers and alter their stability properties at will.

As we show in Sec. III, the introduction of such a multiplicative driving term does not affect at all the space-time separability of the equations of motion and hence may be easily employed to construct DB's, whose frequencies are multiples of the driving frequency ω_d. We may also change the DB stability properties, by varying the amplitude of the driving ϵ to force a pair of eigenvalues of the monodromy matrix to enter (or exit) the unit circle, thus making the DB stable (or unstable) under small perturbations.

When a DB is stable, we find large regions of initial conditions around it leading to *quasiperiodic* breathers, which are observed to be stable for as long as we were able to integrate the equations of motion. As we explain in Sec. IV, these represent modulations by a second frequency of the DB lying at the center of these regions and are characterized by a clearly discrete spectrum. At some distance from the DB, the quasiperiodic breathers become unstable, breaking down after relatively short times, through delocalization and energy sharing among all particles.

Stable quasiperiodic breathers with similar properties are also found around the equilibrium position where all particles are at rest. However, as we move away from this point, choosing initial conditions on a two-dimensional Poincaré map of the temporal motion of each particle, we observe near the boundary of a major chaotic layer that the quasiperiodic motion breaks down into chaotic oscillations, which nevertheless remain highly localized. They assume the form of what we may call a *chaotic* breather, as the largest amplitude oscillations begin to wander erratically among a small number of central particles of the lattice.

These oscillations possess an evidently broad banded Fourier spectrum and give the impression that the breather "dances" chaotically over a part of the lattice that never exceeded ten particles in all our simulations. Thus, our chaotic breathers differ from those found in the literature [18–21], since they do not travel over the full extent of the lattice and, more importantly, are not seen to collapse through energy equipartition, for as long as we were able to observe them. We argue, therefore, that their localization is due to the absence of resonances with phonons, since our lattices are free from linear dispersion. In Sec. V, we present similar results on quasiperiodic breathers starting with different DB profiles and selecting different parameters of the problem, corresponding to what is referred to as "hard" and "soft" DB's in the literature [29].

Of course, the complete absence of linear dispersion is rare in realistic systems. What one may encounter, however, in physical models is linear coupling terms, with a small coefficient $c>0$. Thus, in Sec. VI, we introduce such terms in our equations of motion and show that for sufficiently small c, stable quasiperiodic breathers around periodic ones continue to persist for very long times, just as in the $c=0$ case. Finally, we point out in our Conclusions that the occurrence of chaotic breathers is a rather delicate phenomenon, as their formation depends crucially on how quasiperiodic breathers destabilize, as we approach a chaotic region of the low-dimensional dynamics governing the class of Hamiltonian lattices studied in this paper.

II. BREATHERS OBTAINED BY COMPLETE SPACE-TIME SEPARATION

We consider a one-dimensional lattice of coupled nonlinear oscillators with unit mass, described by the Hamiltonian

$$H=\sum_n\left\{\frac{1}{2}\dot{u}_n+\frac{1}{2}u_n^2-\frac{1}{4}u_n^4+\frac{K}{4}(u_{n+1}-u_n)^4\right\} \tag{4}$$

[see Eqs. (1) and (3)], where n varies from $-\infty$ to $+\infty$ and K is a positive constant. We point out the absence of quadratic coupling terms in Eq. (4) and hence the lack of linear dispersion in our model. The equation of motion for the nth oscillator is thus given by

$$\ddot{u}_n=K(u_{n+1}-u_n)^3+K(u_{n-1}-u_n)^3-u_n+u_n^3. \tag{5}$$

It has been shown for this system [4,23,29] that there is a class of solutions which can be written as a product of a purely spatial (n-dependent) part and a function of time only as follows:

$$u_n(t) = \Phi_n G(t), \tag{6}$$

where Φ_n corresponds to the spatial profile of the solution and $G(t)$ describes its time evolution. This can be easily seen by substituting Eq. (6) in the equation of motion (5) and writing it as an equality between an expression that depends only on n and one that is solely time dependent. Equating both of these expressions to a constant C, one thus finds that $G(t)$ satisfies the (autonomous) Duffing equation

$$\ddot{G} + G = -CG^3, \tag{7}$$

while the spatial part of the solution obeys the second-order recursion relation

$$C\Phi_n + K(\Phi_{n+1} - \Phi_n)^3 + K(\Phi_{n-1} - \Phi_n)^3 + \Phi_n^3 = 0. \tag{8}$$

Note that (8) describes a second-order mapping that can be solved uniquely for Φ_{n+1} and $\Psi_{n+1} = \Phi_{n+1} - \Phi_n$ in terms of Φ_n and Ψ_n. In fact, it is invertible, as it can also be solved uniquely for Φ_n and Ψ_n in terms of Φ_{n+1} and Ψ_{n+1}. Clearly, the only thing that matters about C is its sign (since C can be scaled out), so we only consider here the cases $C=1$ and $C=-1$ separately. We also fix $K=1$ everywhere throughout this paper.

Of course, there are many different kinds of solutions of the mapping (8) (e.g., fixed points, periodic, etc.) and hence also of the lattice (6) that one may wish to construct by combining them with the appropriate solution of Eq. (7). Here, we are interested in finding discrete breathers of this lattice—i.e., spatially localized, time-periodic solutions of a prescribed frequency ω_b [2,5,8,9]. One very efficient method for computing their spatial profile is by finding the homoclinic orbits located at the intersections of the invariant manifolds of the saddle point at the origin of map (8) as shown in [30–32]. One may thus select among these orbits any profile one wishes, having the required symmetry, number of local extrema, etc. The exact breather solution is then calculated as the product of this homoclinic orbit with the periodic solution of Eq. (7) having the desired frequency ω_b [29]. Let us choose, for example, one of the simplest such profiles corresponding to a symmetric breather with a single central maximum shown in Fig. 1.

We shall first set $C=1$, which corresponds to the case where the Eq. (7) has periodic solutions for *all* initial displacements $G(0)$ and $\dot{G}(0)$, as it possesses an everywhere positive-definite potential. For $C=1$ the frequency of a periodic solutions is larger than the equilibrium frequency of the potential $[\omega_b > \omega_0 = V''(0) = 1]$ and neighboring particles are oscillating out of phase (see Fig. 1). This behavior appears in systems with hard on-site potential and gives rise to DB's called "hard breathers" [29].

All we have to do now to construct such DB solutions is choose, on the phase plane of Duffing's equation, a point $G(0)=D$ and $\dot{G}(0)=0$ corresponding to a periodic orbit with frequency ω_b, select a particular homoclinic orbit of the map (8), and multiply them to obtain the initial profile $u_n(0) = D\Phi_n$ of a DB having zero initial velocities and oscillating with the same frequency. For example, for the breather of Fig. 1, we plot the evolution of the central particle as a function of time in Fig. 2(a) and note that increasing D increases the frequency of the breather, in a manner shown in Fig. 2(b).

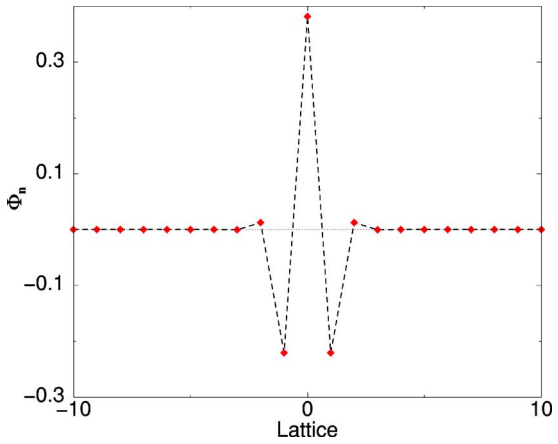

FIG. 1. (Color online) The profile Φ_n of a simple breather of the autonomous system (7) for $C=1$, $K=1$.

Having shown how to construct exact breathers, we now come to the question of the stability of their time evolution under small perturbations of their initial conditions. Since these solutions are periodic, Floquet analysis can be invoked to study stability through the calculation of the eigenvalues of the monodromy matrix (Floquet multipliers) of the associated linear variational problem [5,8,9,31,32]. This analysis reveals, in the case of the profile of Fig. 1, that this breather is unstable, since it has one pair of monodromy eigenvalues outside the unit circle, $\lambda_1 > 1$, $\lambda_2 = 1/\lambda_1 < 1$. In fact, this instability becomes even stronger for larger D (and larger fre-

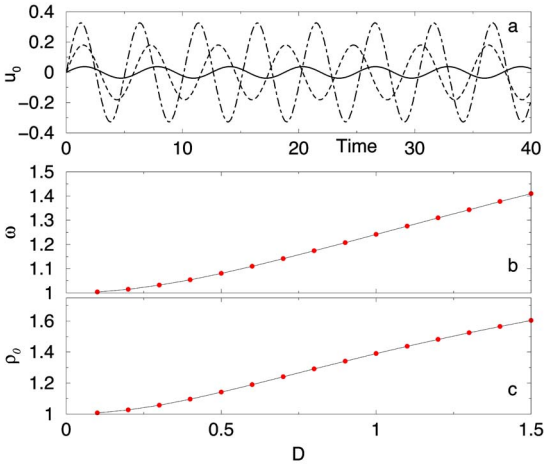

FIG. 2. (Color online) (a) The time evolution of the central particle of the breather of Fig. 1. The solid line corresponds to $D=0.1$, dashed line to $D=0.5$, and dot-dashed line to $D=1.0$ (time in dimensionless units). (b) The breather frequency as a function of the parameter D. (c) The magnitude of the single Floquet multiplier $\lambda_1 > 1$ as a function of D.

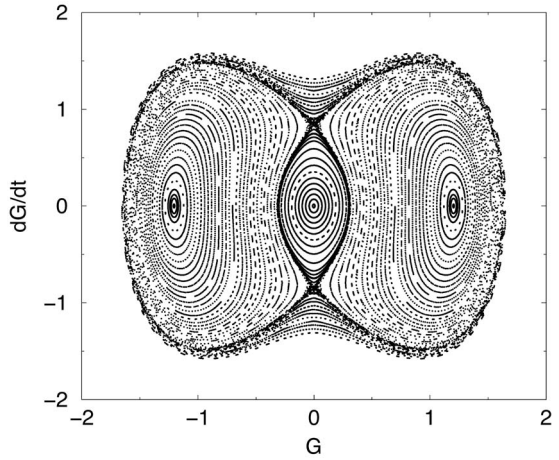

FIG. 3. Poincaré surface of section for Duffing's equation with parametric driving $\epsilon=0.7$ and $\omega_d=2.6355$.

quencies), as seen by the monotonic increase of the magnitude of the real Floquet multiplier $\lambda_1>1$, plotted as a function of D in Fig. 2(c).

III. CONTROLLING THE STABILITY OF BREATHERS BY PARAMETRIC DRIVING

The question, therefore, naturally arises: Is it possible to devise an appropriate control mechanism by which stable breathers can be found for this system? One way by which this can be done is to introduce a parametric driving term in the factor multiplying the harmonic part of the on site potential of all oscillators. To this end, we propose to add to the coefficient of the harmonic term of the on site potential (3) a periodic modulation, thus changing the equation of motion to

$$\ddot{u}_n = K(u_{n+1}-u_n)^3 + K(u_{n-1}-u_n)^3 - [1-\epsilon\cos(\omega_d t)]u_n + u_n^3, \tag{9}$$

where ϵ and ω_d represent the amplitude and frequency of the driver. We have chosen this modification for two reasons: first because it is physically meaningful, as such a type of parametric driving can be experimentally implemented, and second because it does not affect the mathematical property of having solutions of the type (6). Thus, separating again the space and time-dependent parts as before, we observe that the Duffing equation (7) now becomes

$$\ddot{G} + [1-\epsilon\cos(\omega_d t)]G = -CG^3, \tag{10}$$

while the spatial profile of the solution can again be constructed independently by solving a mapping equation identical to Eq. (8). Thus, we can study breather solutions of our lattice by selecting points $G(t_i)$ and $\dot{G}(t_i)$ on the surface of section of Eq. (10) at times $t_i=2i\pi/\omega_d$ (i is an integer) and combining the corresponding solution $G(t)$ with the spatial profile Φ_n given by Eq. (8). In Fig. 3, we exhibit a global picture of the dynamics of such a Poincaré map for $\epsilon=0.7$ and $\omega_d=2.6355$.

We may choose, for example, a driving frequency ω_d equal to a multiple of the desired frequency of the breather ω_b, $\omega_d=k\omega_b$ (k is an integer), and look for that breather at the center of a chain of k islands, on the surface of section of Fig. 3. As is evident from this figure, there are two big islands corresponding to a resonance of twice the period (and half the frequency) of the driving, whose centers are located at the points $D_c=\pm 1.2043$ on the horizontal axis. They correspond to a period-2 orbit of the Poincaré map and hence provide initial amplitudes for DB's oscillating with $\omega_b=2\omega_d$. Clearly, the origin of the figure at (0,0) is an equilibrium point of Eq. (10), where the lattice is at rest. Two interesting questions arise therefore with respect to this figure.

(i) What type of lattice oscillations do we obtain if we choose our initial conditions on one of the quasiperiodic orbits of Eq. (10) encircling the origin or one of the period-2 points? Do they lead to some form of quasiperiodic breathers and are these stable under small perturbations in their time evolution?

(ii) What about initial conditions chosen within the chaotic layer surrounding the origin in Fig. 3? Can they yield some form of chaotic breathers?

To find out, let us start by choosing a point at the center of the two large islands of Fig. 3 as an initial value for the lattice displacements and construct a DB with $\omega_b=2\omega_d$, using the Φ_n profile of Fig. 1. In particular, we take as our starting point the center of the island on the right, $(D,0)$, whence the initial conditions for our lattice are $u_n(0)=D\Phi_n$ and $\dot{u}_n(0)=0$. Using Newton's method, we now calculate the exact DB for the lattice and compute its Floquet multipliers. We have used throughout this paper a lattice of $N=32$ particles, which is quite sufficient for our calculations, as shown clearly by the picture of Fig. 1.

In the limit $\epsilon=0$ we have already seen that this breather is unstable with a single pair of Floquet multipliers lying outside the unit circle. Increasing ϵ, however, we observe that the breather undergoes a codimension-1 bifurcation: The two real multipliers move towards the unit circle and as ϵ becomes larger than some critical value ϵ_c they enter the unit circle and the breather becomes stable. Thus, using this form of periodic driving control is possible and the breather is stabilized. The magnitudes and arguments of the Floquet multipliers λ_i closest to +1 are shown in Fig. 4, for $C=1$ and $\omega_d=2.6355$. The critical value of the driving in this case is $\epsilon_c=0.6675$.

IV. QUASIPERIODIC AND CHAOTIC BREATHERS

We have thus discovered that, when $\epsilon>\epsilon_c$, a stable periodic breather is obtained starting from the center of the big island on the right of Fig. 3, $(D_c,0)$. Suppose now that we perturb this initial condition by placing our starting point at a distance $G(0)=D=D_c-\delta$, $\delta>0$, away from the center of the island (always with zero initial velocities), with δ small enough that D remains inside the island. What about the corresponding solutions of the lattice? We may expect that for small δ they will have the form of quasiperiodic breathers and also be *stable* for two reasons: They lie on tori of quasiperiodic motion around a stable periodic orbit of an N-degrees-of-freedom Hamiltonian system [11] and are free from phonon resonances due to the absence of linear disper-

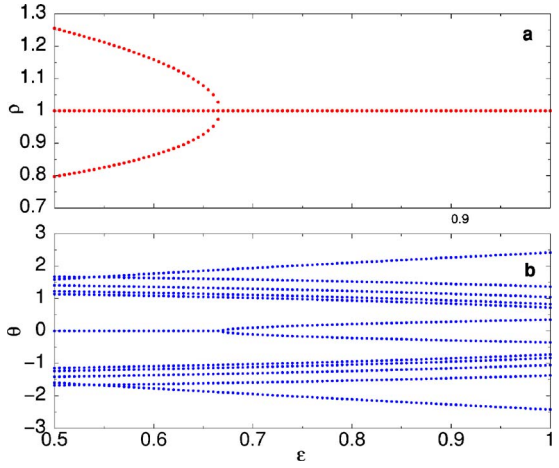

FIG. 4. (Color online) (a)The magnitude of the two real Floquet multipliers λ_1, λ_2 becomes 1 by an inverse bifurcation as ϵ exceeds the value $\epsilon_c = 0.6675$. (b) The arguments θ_i of the Floquet multipliers λ_i closest to +1, as functions of the parametric driving ϵ.

sion. But how far can we go from the center of the island before the dynamics becomes unstable?

To answer these questions, we vary $G(0) = D$ and observe indeed the occurrence of stable quasiperiodic breathers, until D reaches approximately half the distance between the center and the edge of the island on the Poincaré map. For example, with $\epsilon = 0.7$, the center of the island is located at $D_c = 1.204\,368$ and its edge is formed by a chaotic layer crossing the positive horizontal axis at about $D_s = 0.313\,739$. Using as initial conditions for the lattice $u_n = D\Phi_n$ with $D > 0.80$, we find quasiperiodic breathers which remain stable for very-long-time simulations. In Figs. 5(a) and 5(b) we plot the oscillations of the central particle for the DB with $\omega_b = 2\omega_d$ ($D = D_c$) and a quasiperiodic breather with $D = 0.8$, respectively. We also find the frequencies involved in the motion of this particle using the Fourier transform [Figs. 5(c) and 5(d), respectively]. Note the presence of a single frequency in the spectrum of Fig. 5(a) plotted in Fig. 5(c) and the occurrence of a discrete spectrum for the quasiperiodic breather of Fig. 5(b) plotted in Fig. 5(d). When $D < 0.80$, however, the quasiperiodic breather becomes unstable, in the sense that it is numerically seen to collapse after relatively short times.

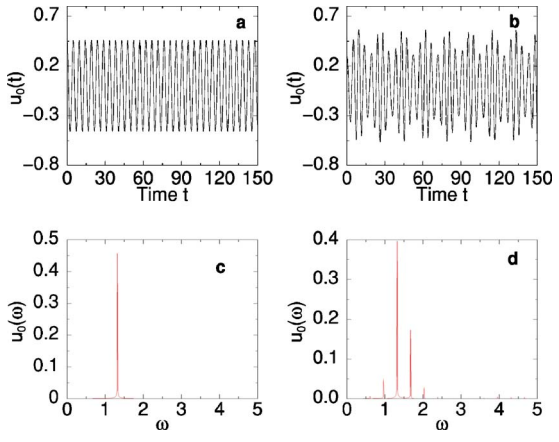

FIG. 5. (Color online) (a) Time evolution of the central breather particle $u_0(t)$ in the center of the island for $D = 1.2043$. (b) The stable quasiperiodic breather inside the island for $D = 0.8$. (c) The Fourier transform of $u_0(t)$ for the stable breather when $D = 1.2043$. (d) The Fourier transform of $u_0(t)$ for the quasiperiodic breather when $D = 0.8$. We have used a lattice of $N = 32$ particles with the parameter values $\epsilon = 0.7$, $\omega_d = 2.6355$, and $C = K = 1$ (time in dimensionless units).

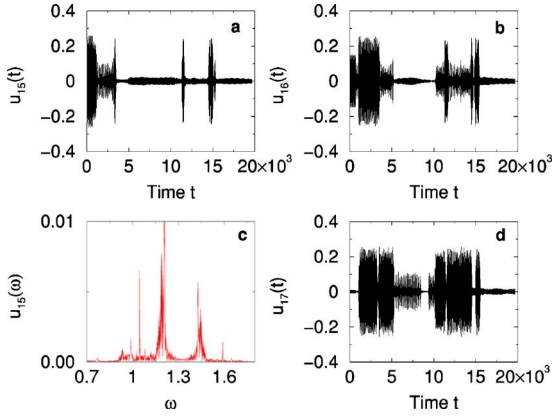

FIG. 6. (Color online) Evidence of a chaotic breather with the initial profile of Fig. 1 and initial conditions (0.313,0) in Fig. 3. (a) Time evolution of the central particle $n = 15$ and (b) its first neighbor $n = 16$. (c) The Fourier transform of (a) shows parts that are clearly broad banded. (d) The energy of the breather in this experiment is seen to be located also for long times in the second neighbor $n = 17$. The lattice parameters are as in Fig. 5 (time in dimensionless units).

Stable quasiperiodic breathers with smaller amplitude can also be observed if the initial condition is placed inside the central island around the origin of Fig. 3. However, starting again with initial conditions $(D, 0)$ and moving to the right of $D = 0$, we do not find that the quasiperiodic breather destabilizes in the same manner as described above. Instead, when we are very close to the chaotic layer joining the two saddle points of the (unstable) period 2 on the $D = 0$ axis of Fig. 3, the breather becomes chaotic. Indeed, as we show in Figs. 6 and 7, starting with $D = 0.313$, the energy of the central particle of the breather, located initially at the site $n = 15$, starts to wander to nearby positions, while the total energy remains localized between the sites $n = 10$ and $n = 20$. The fact that the oscillations are truly chaotic is evidenced by the Fourier spectrum of the $n = 15$ particle, for example, which is shown in Fig. 6(c) to exhibit a clearly broadbanded part.

In fact, following the oscillations of this breather in time we observe that it "dances" chaotically in space, as the location of its maximum amplitude shifts unpredictably from the left to the right of the center particle at $n = 15$ and vice versa (see Fig. 7). We emphasize that for as long as we have been able to follow its evolution, the oscillations remained localized within a small number of particles around the center (between $n = 10$ and $n = 20$), while the rest showed very little appreciable movement.

Varying the frequency and/or the strength of the parametric driving, one can, of course, find additional stable periodic breathers, whose initial conditions lie at the centers of islands with higher periodicity. As an example, we mention

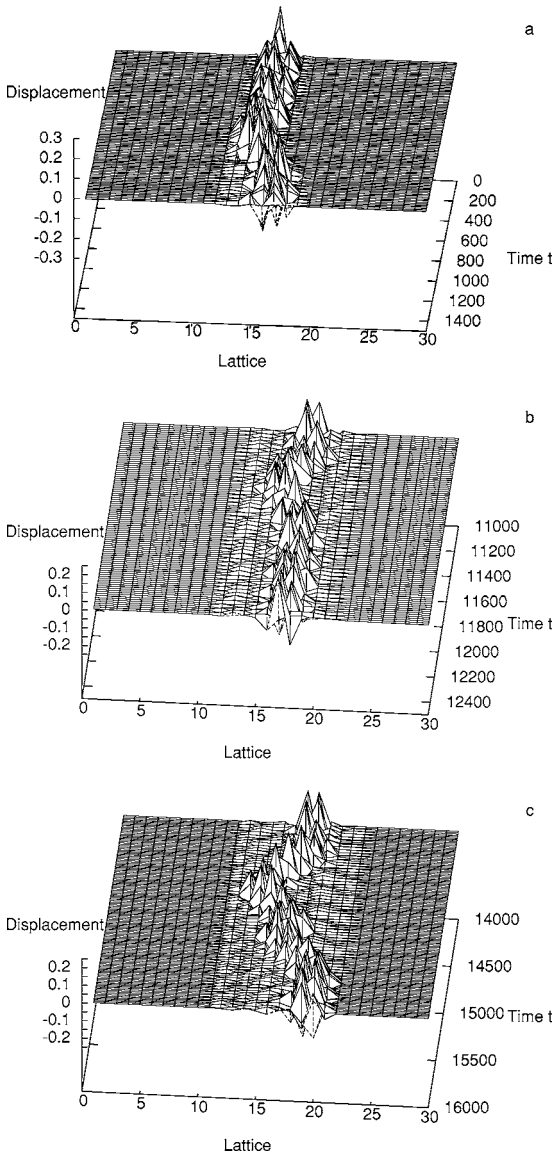

FIG. 7. (a) Three-dimensional time evolution of the chaotic breather for $0<t<1500$. (b) Three-dimensional time evolution of the chaotic breather for $11\,000<t<12\,500$. (c) Three-dimensional time evolution of the chaotic breather for $14\,000<t<16\,000$ (time in dimensionless units).

that for $\omega_d=4.8$ and $\epsilon=0.5$, one finds that there is a group of four islands on a surface of section similar to that of Fig. 3: The center of each island is on one of the main axes, two at $y=0$ and $x=\pm D$ and two at $x=0$ and $y=\pm D$, with $D=0.7526$. Using any one of these as a starting point together with the Φ_n values of Fig. 1, we find a stable periodic breather with frequency $\omega=1.2=\omega_d/4$, as expected. Small deviations from the center of these islands lead to quasiperiodic breathers.

V. BREATHERS WITH A DIFFERENT SPATIAL PROFILE

A. Hard breathers

The breather profile we have studied so far, shown in Fig. 1, is often called "hard" due to the fact that $C=1$ in Eq. (7)

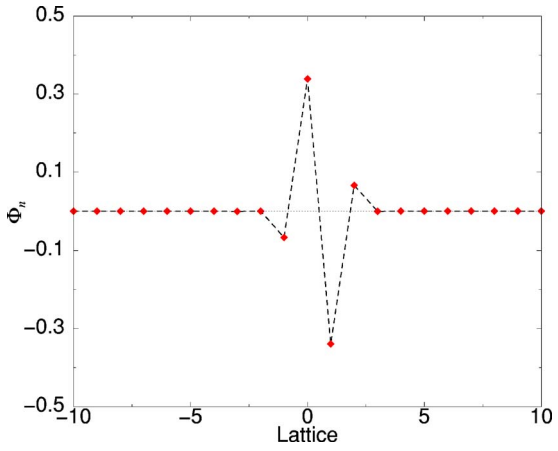

FIG. 8. (Color online) The breather profile Φ_n of an antisymmetric breather for $C=1$ and $K=1$.

corresponds to a $G(t)$ potential that is everywhere positive definite. It is also "even" (or symmetric) with respect to the central particle. It would therefore be interesting to carry out a similar investigation for a different spatial profile—for example, one that is "odd" or *antisymmetric*, with respect to the central particle. In Fig. 8 we plot the spatial profile Φ_n of such a breather.

Using Floquet stability analysis we find that this configuration is in fact linearly stable in the absence of parametric driving. When we introduce the driving, the mode remains stable if the amplitude of the forcing term ϵ remains smaller than some critical value ϵ_c. For example, taking as the frequency of the driver $\omega_d=2.6355$, we find that this critical value is $\epsilon_c=0.822$. To see this, we plot in Fig. 9 the magnitude and argument of the Floquet multipliers ($\lambda_i=\rho_i e^{i\theta_i}$) as a function of the amplitude ϵ of the driving force. Comparing with Fig. 4, we see that a "forward" bifurcation takes place here, as two multipliers become real for $\epsilon>\epsilon_c=0.822$, with $\lambda_1>1$ being responsible for the breather's instability. From these two figures we also conclude that there is an interval of

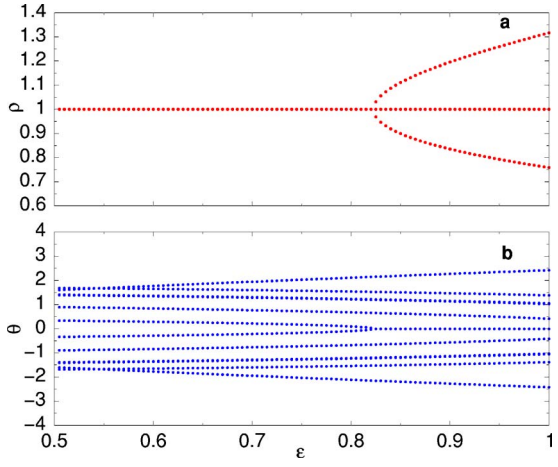

FIG. 9. (Color online) The amplitude ρ_i (a) and the argument θ_i (b) of the Floquet multipliers of the antisymmetric breather as a function of the driver's amplitude ϵ. The parameters are $C=1$, $K=1$, and $\omega_d=2.6355$.

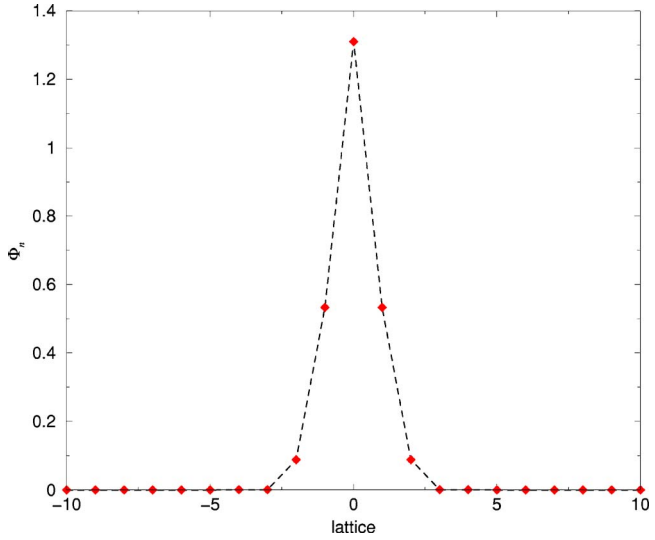

FIG. 10. (Color online) The soft breather profile Φ_n for $C=-1$ and $K=1$.

forcing amplitudes $0.6675<\epsilon<0.822$ where both symmetric and antisymmetric breathers are stable.

Using now the spatial profile Φ_n of the antisymmetric breather of Fig. 9 and $(D,0)$ from Fig. 3 to form the initial conditions for the lattice, $u_n(0)=D\Phi_n$ and $\dot{u}_n(0)=0$, we integrate numerically the equations of motion (9) and follow the solutions (6) for long times. If we choose $\epsilon=0.7$ and $D=1.204\,368$, at the center of the islands, then the solution yields a stable DB. Small deviations from this point lead again to stable quasiperiodic breathers as in the symmetric case of the previous section. Moving away from the center of the island towards (0,0), these quasiperiodic oscillations cease to be localized and become unstable when D reaches the critical value $D_c=0.874$. Comparing this critical value with the one of the symmetric breather (which is $D_c=0.8$), we conclude that the size of the regions corresponding to stable quasiperiodic breathers is smaller for the antisymmetric breather of Fig. 8 than it is for the symmetric one of Fig. 3.

B. Soft breathers

We can perform exactly the same investigation as above in the case of a lattice with "soft" breathers by setting $C=-1$ in the Duffing equations (7) and (10), as well as the mapping (8), which now yields the symmetric breather profile shown in Fig. 10.

Thus, either solving for the homoclinic orbits of Eq. (8) or starting with an approximation of the breather profile of Fig. 10 and using Newton's method to converge to the exact solution [3], we were able to find stable soft breathers, with frequency $\omega_b=0.95$, choosing initial conditions at the centers of the big islands of Fig. 11, which represents the surface of section of Eq. (10) for $\omega_d=1.9$ and $C=-1$ (see also Fig. 3). The behavior of the Floquet multipliers as functions of the amplitude of the periodic forcing ϵ is shown in Fig. 12. Beginning with perturbations around the period-2 points yields again stable quasiperiodic breathers up to relatively large distances away from the centers of the island, as in the case of the hard breathers with $C=1$ described above.

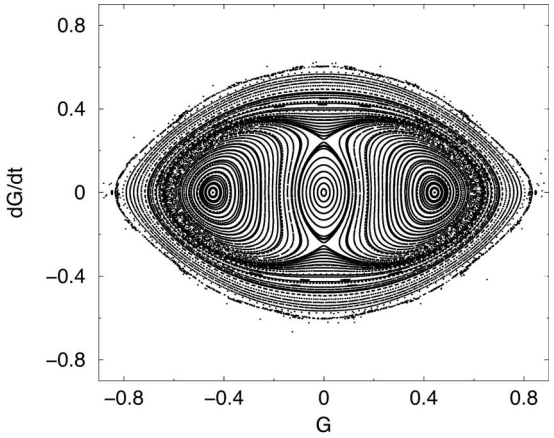

FIG. 11. The Poincaré map of the parametrically driven Duffing's equation (10), with $\epsilon=-0.1$, $\omega_d=1.9$, $C=-1$, and $K=1$. The center of the right big island is at $D=0.4435$.

Interestingly enough, the quasiperiodic orbits observed in this case appear to be stable even for initial conditions chosen close to the separatrix around the origin of Fig. 11. In fact, even when we chose $D=0.35$ and $D=0.2$, the breather was stable for as long as we could integrate, with oscillations whose envelope exhibits long period modulations [see Figs. 13(b) and 13(c)] and a discrete Fourier spectrum, whose main part is concentrated around the frequency $\omega_b=0.95$ of the DB of Fig. 13(a) [see Figs. 13(d)–13(f)].

Finally, if we select initial conditions with even smaller value of D, closer to the chaotic layer encircling the origin of Fig. 11, we eventually find unstable quasiperiodic breathers, which become delocalized after relatively short time periods. A similar situation holds if we approach the chaotic layer starting from (0,0). Even though we performed detailed computations, taking small increments in our D values, we were not able to find chaotic breathers for $C=-1$, as we did in the

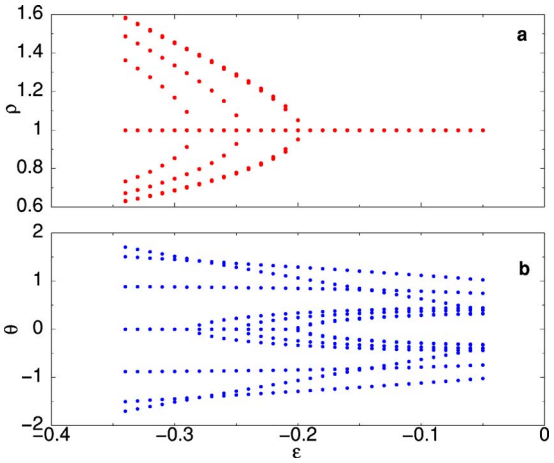

FIG. 12. (Color online) (a) The magnitudes and (b) the arguments of the Floquet multipliers λ_i, $i=1,2,\ldots$, of the soft breather as functions of the amplitude of the periodic forcing ϵ, as they bifurcate off the unit circle at $\epsilon<\epsilon_c=-0.2$, with $\omega_d=1.9$.

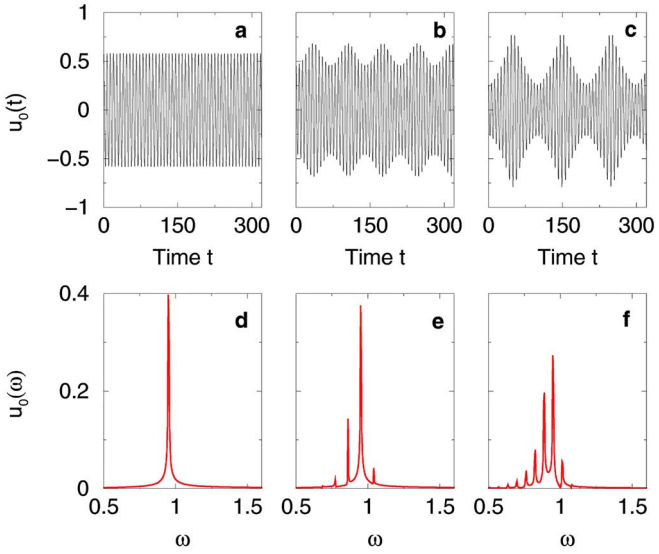

FIG. 13. (Color online) The time evolution and the Fourier transform of the central breather particle for $\epsilon=-0.1$ and $\omega_d=1.9$. Upper panels: (a) Periodic breather with initial condition $D=0.4435$ at the center of the right big island of Fig. 11. (b) Quasiperiodic breather with $D=0.35$. (c) Quasiperiodic breather with $D=0.2$, close to the separatrix of Fig. 11. Lower panels: (d) Fourier transform of (a). (e) Fourier transform of (b). (f) Fourier transform of (c). (time in dimensionless units).

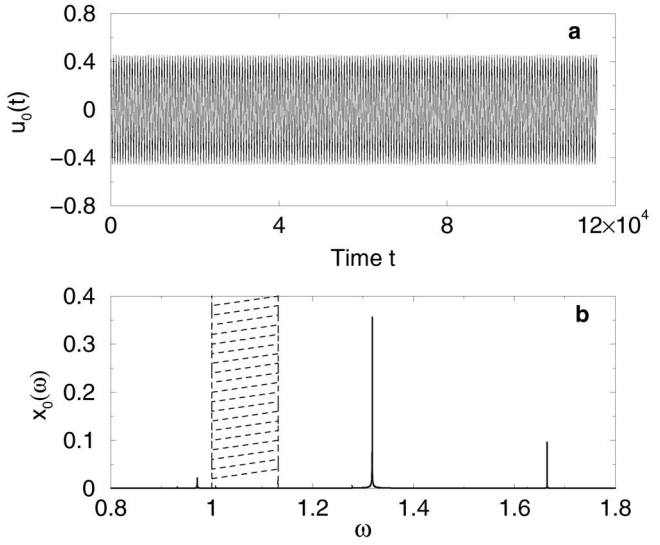

FIG. 14. The temporal evolution and Fourier transform of the quasiperiodic hard breather in the presence of weak linear dispersion with $c=0.07$, $\epsilon=0.7$, and $\omega_d=2.6355$ (time in dimensionless units). (a) The temporal evolution of the central particle of the breather. (b) The Fourier transform of the evolution of the central particle (the dashed lines indicate the location of the phonon band).

$C=1$ case. In all our experiments with soft solutions, the quasiperiodic breathers become unstable when we reach the chaotic layer and localization was lost without the formation of chaotic breathers.

VI. EFFECT OF LINEAR DISPERSION

Evidently, the absence of linear dispersion in our system appears to be responsible for the existence and stability of quasiperiodic and chaotic breathers since the linear modes have zero group velocity and have all the same frequency (i.e., the rest frequency of the on-site potential) and hence cannot propagate energy. Therefore, to further study their effect on the localization phenomena we have observed, let us introduce a small harmonic term in the interaction potential, $V_c(x)=cx^2/2$, due to which a band of linear modes is formed with the usual dispersion relation and nonzero group velocity $\omega^2(q)=\omega_0^2+4c\sin^2(q/2)$ ($\omega_0=1$ is the rest frequency of the on-site potential V).

This means that if any of the harmonics of the breather frequencies lie within this band, energy will be dissipated through phonons and the breather will decay. In the case of a quasiperiodic breather there are at least two characteristic frequencies (ω_1 and ω_2, which are intrinsic to the breather). Since these two frequencies are incommensurate, there will exist internal frequencies of the breather of the form $\omega=n_1\omega_1+n_2\omega_2$ with n_1 and n_2 integers, which will lie within the phonon band causing the breather to lose energy. The rate at which this will happen will be lower for large n_1 and n_2 (since the equivalent Fourier coefficients of the breather will also be very small). Of course, for a very narrow phonon band and for breather frequencies close to each other, the integer numbers n_1 and n_2, which produce a frequency ω inside the band will be very large, and therefore, the quasiperiodic breather is expected to have a very large lifetime.

In Fig. 14 we show the time evolution and the Fourier transform of the central particle of the hard quasiperiodic breather in the presence of weak linear dispersion. The amplitude and the frequency of the parametric driver are the same as in Fig. 5. A small linear term V_c has been included in the nearest-neighbor interaction, and the coupling parameter is $c=0.07$. Clearly, because of the linear interaction, we can no longer separate the spatial and temporal parts of the solution, but the exact periodic breather can be calculated numerically using Newton's method. Small excitations around this periodic solution are then found to lead to solutions with quasiperiodic behavior which persists for very long times ($t>10^5$). As can be seen in Fig. 14, after $t=1.2\times10^5$ time units the quasiperiodic breather still shows no visible loss of energy.

Even though in the presence of a linear interaction the spatial and temporal components of the solution cannot be exactly separated, for very small coupling strength $c>0$ we can still describe the behavior of the system in terms of two-dimensional phase-space maps of Eq. (10). An exact periodic breather is again found to exist at the center of the island, with frequency $\omega_b=\omega_d/n_d$ (where n_d is the rotation number corresponding to the island).

As shown in Fig. 15, the linear stability of the breather at the center of the island is preserved for nonzero values of the parameter c. As the coupling increases, however, the Floquet multipliers collide with each other on the unit circle and instabilities appear. The first such instability though appears for a relatively large value of the coupling (i.e., $c=0.09$). It is also interesting to note that if the central periodic breather of

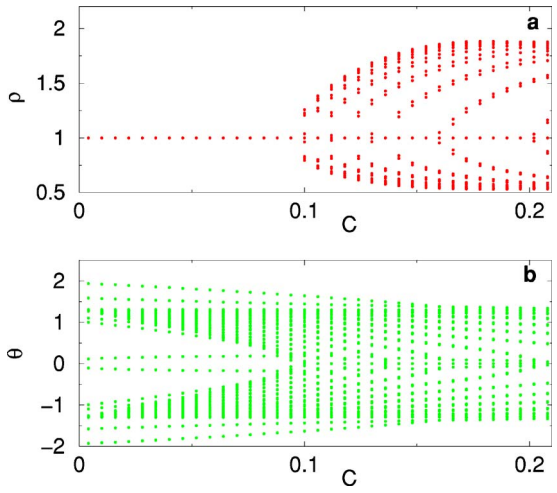

FIG. 15. (Color online) The Floquet multipliers as a function of the linear dispersion parameter c for the exact periodic breather with $\epsilon=0.7$ and $\omega_d=2.6355$. (a) The magnitude ρ of the Floquet multipliers as a function of c and (b) the argument θ of the Floquet multipliers as a function of c.

Figs. 14 and 15 in the absence of parametric driving is unstable, we can use the parametric driver to realize its stabilization. Thus, we believe that the results of this paper can be used in more general situations to produce stable periodic and quasiperiodic breathers in systems where the linear dispersion terms are small enough.

VII. CONCLUSIONS

In this paper, we have studied breather dynamics in a one-dimensional lattice with only quartic nearest-neighbor interactions—i.e., in the absence of linear dispersion terms. Our goal was to study the properties of the lattice when there is no phonon spectrum to cause the breakdown of breathers via the mechanism of resonances with linear coupling terms. Our main result is that, in the absence of such terms, localization is indeed a robust property, as quasiperiodic and even chaotic breathers are observed to remain spatially localized, for as long as we were able to integrate the equations of motion.

We have characterized our breathers as quasiperiodic or chaotic depending on whether their Fourier spectrum is, respectively, discrete or broadbanded. In fact, we have observed in all our investigations a strong resemblance of the infinite-dimensional lattice with what one expects from a Hamiltonian system with only a finite number of degrees of freedom. This is, of course, not surprising, as in all our solutions only a very small part of the lattice is seen to take part in the dynamics. Thus, we may think of DB's as simple periodic orbits of an N-degrees-of-freedom Hamiltonian, surrounded by N-dimensional tori, on which the motion remains confined, forever, since there are no phonon resonances to destroy them.

Their localization in space strongly suggests that they share the topological properties of the central DB about which they oscillate and that the full dynamics actually occurs on a very-low-dimensional part of the $2N$-dimensional phase space. This is further supported by the fact that even the chaotic regions in that subspace are of low dimensionality as they are seen to contain chaotic motion which is limited to a very small number of particles for very long times.

To date, a number of realistic lattice systems have been reported in the literature [25–27], where the nonlinear dispersion is dominant and the linear dispersion is very small, and which can be considered as being nearly free from linear dispersion. For this reason, we investigated in Sec. VI of this paper the effect of adding a small linear dispersion term to our lattices. We were thus able to demonstrate that, for small enough values of the linear coupling coefficient $c>0$ and long enough times, stable periodic breathers with large regions of stable quasiperiodic breathers around them still exist, with properties that can be controlled by methods very similar to the ones we used in the $c=0$ case.

Finally, it would be important to examine the effect of *long-range* interactions on such quasiperiodic and chaotic breathers, as has been recently done for the DB solutions of these lattices [29]. Thus, one would be able to test whether there also exist similar characteristic crossover lengths destroying localization of quasiperiodic and chaotic oscillations and compare the results with analogous phenomena observed in the case of localized periodic oscillations.

ACKNOWLEDGMENTS

Special thanks are due to S. Flach, A. Gorbach, and M. Johansson for many interesting discussions on the contents of this paper. T.B. is particularly indebted to the Max-Planck-Institut für Physik Komplexer Systeme, in Dresden, for its hospitality during March–June 2005, when most of this work was carried out. He also thanks the European Social Fund (ESF), Operational Program for Educational and Vocational Training II (EPEAEK II) and particularly the programs HERAKLEITOS and PYTHAGORAS II, for partial support.

[1] A. J. Sievers and S. Takeno, Phys. Rev. Lett. **61**, 970 (1988); S. Takeno, J. Phys. Soc. Jpn. **59**, 1571 (1990).
[2] R. S. MacKay and S. Aubry, Nonlinearity **7**, 1623 (1994).
[3] J. L. Marin and S. Aubry, Nonlinearity **9**, 1501 (1994).
[4] S. Flach, Phys. Rev. E **50**, 3134 (1994).
[5] S. Aubry, Physica D **103**, 201 (1997).
[6] Ding Chen, S. Aubry, and G. P. Tsironis, Phys. Rev. Lett. **77**, 4776 (1996).
[7] K. O. Rasmussen, S. Aubry, A. R. Bishop, and G. P. Tsironis, Eur. Phys. J. B **15**, 169 (2000).
[8] S. Flach and C. R. Willis, Phys. Rep. **295**, 182 (1998).
[9] S. Flach and A. V. Gorbach, Int. J. Bifurcation Chaos Appl. Sci. Eng. (to be published).
[10] M. J. Ablowitz and P. A. Clarkson, *Solitons, Nonlinear Evolu-*

tion Equations and Inverse Scattering, Lecture Note Series, Vol. 149 (Cambridge University Press, Cambridge, England 1991).
[11] C. Antonopoulos, T. Bountis, and Ch. Skokos, Int. J. Bifurcation Chaos Appl. Sci. Eng. (to be published).
[12] S. Flach, M. V. Ivanchenko, and O. I. Kanakov, Phys. Rev. Lett. **95**, 064102 (2005).
[13] G. P. Berman and F. M. Izrailev, Chaos **15**, 015104 (2005).
[14] M. Johansson and S. Aubry, Nonlinearity **10**, 1151 (1997).
[15] D. Bambusi and D. Vella, Discrete Contin. Dyn. Syst., Ser. B **2**, 389 (2002).
[16] P. G. Kevrekidis and M. I. Weinstein, Physica D **142**, 142 (2000).
[17] P. G. Kevrekidis and M. I. Weinstein, Math. Comput. Simul. **62**, 65 (2003).
[18] Y. A. Kosevich and S. Lepri, Phys. Rev. B **61**, 299 (2000).
[19] K. Ullmann, A. J. Lichtenberg, and G. Corso, Phys. Rev. E **61**, 2471 (2000).
[20] V. V. Mirnov, A. J. Lichtenberg, and H. Guclu, Physica D **157**, 251 (2001).
[21] T. Dauxois, R. Khomeriki, F. Piazza, and S. Ruffo, Chaos **15**, 015110 (2005).
[22] J. C. Comte, Phys. Rev. E **65**, 067601 (2002).
[23] Y. S. Kivshar, Phys. Rev. E **48**, R43 (1993).
[24] P. Tchofo Dinda, T. C. Kofane, and M. Remoissenet, Phys. Rev. E **60**, 7525 (1999).
[25] P. Rosenau and James M. Hyman, Phys. Rev. Lett. **70**, 564 (1993); P. Rosenau, *ibid.* **73**, 1737 (1994); P. Rosenau and S. Schochet, *ibid.* **94**, 045503 (2005).
[26] A. S. Kovalev and M. V. Gvozdikova, Low Temp. Phys. **24**, 484 (1998).
[27] S. Dusuel, P. Michaux, and M. Remoissenet, Phys. Rev. E **57**, 2320 (1998).
[28] B. Dey, M. Eleftheriou, S. Flach, and G. P. Tsironis, Phys. Rev. E **65**, 017601 (2002).
[29] A. V. Gorbach and S. Flach, Phys. Rev. E **72**, 056607 (2005).
[30] T. Bountis *et al.*, Phys. Lett. A **268**, 50 (2000).
[31] J. Bergamin, T. Bountis, and M. Vrahatis, Nonlinearity **15**, 1603 (2002).
[32] J. M. Bergamin and T. Bountis, Suppl. Prog. Theor. Phys. **186**, 330 (2003).